Fast Wideband Electromagnetic Analysis Using the Interpolation Technique and Fast Generating Matrix Method

Wei Bin Kong [1,2], Xiao Fang Yang [1], Feng Zhou [1], Jia Ye Xie [3], Ru Gang Wang [1], and Kai Lai Zheng [4]

[1] College of Information Engineering
Yancheng Optical Fiber Sensing and Application Engineering Technology Research Center
Yancheng Institute of Technology, Jiangsu Yancheng, 224051, China
kongweibin2007@sina.com,

[2] State Key Laboratory of Millimeter Waves
Southeast University, Jiangsu Nanjing, 210096, China

[3] Industrial Center
Nanjing Institute of Technology, Jiangsu Nanjing, 211167, China

[4] College of Electronic and Optical Engineering & College of Microelectronics
Nanjing University of Posts and Telecommunications, Jiangsu Nanjing, 210023, China

Abstract ─ A fast wideband electromagnetic scattering analysis method based on the interpolation technique and fast generating matrix method is proposed. By factoring out the dominant phase term, the matrix element is transformed into the element which fluctuates slowly with frequency. The matrices over the frequency band are fast generated via interpolation technique. Instead of employing different meshing grids at different frequencies, this new method requires only one mesh generated at the highest frequency of the given bandwidth. This approach not only saves much work in geometrical modeling but also leads to less time for wideband scattering problem. The proposed algorithm is implemented in the platform of FGG-FG-FFT, which is not sensitive to both the grid spacing and the expansion order. A method for fast generating matrix also is introduced to speed up filling the near matrix. Consequently, it can not only reduce the impedance matrix filling time in the whole frequency band but also accelerate the matrix filling process at frequency interpolation sampling points. Several numerical examples are provided to demonstrate the correctness and the efficiency of the proposed method for the wideband scattering analysis.

Index Terms ─ Electromagnetic scattering, FGG-FG-FFT, frequency sweeps, interpolation technique, near matrix.

I. INTRODUCTION

Wideband electromagnetic (EM) scattering analysis has been widely applied to the area of noncooperative radar target identification and radar imaging. Since frequency sweep is always needed in these applications, one has to calculate the scattering at a number of frequency sample points in a given bandwidth. For the analysis of electrically large objects, even a single calculation is very time-consuming, let alone one has to calculate many times. Therefore, it is urgent to accelerate the process of wideband electromagnetic analysis.

Integral equation combined with the method of moments (MoM) is one of the most popular method in computational electromagnetic [1]. In order to overcome the shortcomings of the method of moments in both computation time and storage memory, many fast algorithms have been developed, such as the fast multipole method (FMM) [2], the multilevel fast multipole algorithm (MLFMA) [3]-[6], and the FFT-based methods (Adaptive integral method (AIM), Precorrected-FFT method (P-FFT), IE-FFT, Fitting the Green's function method (FGG-FG-FFT), etc. [7]-[12]). When analyzing broad-band electromagnetic characterristics of the target, the features of the fast algorithms are different. The FMM is based on the addition theorem of Green's function. Therefore, there exists the sub-wavelength breakdown [13]. The FFT-based methods can be applied to all over frequency band [8], [9]. However, one still has to calculate the scattering at each frequency sample point for frequency sweep. Besides the computational load, different meshes are required for different frequencies. This leads to tremendous work in geometrical modeling. In order to save time for preliminary treatment, the surface of the PEC object

Submitted On: June 18, 2018
Accepted On: October 4, 2018

is discretized with triangular patches at the highest frequency. The discrete grid is scale-changing in the whole frequency band. Therefore, a single fast multipole method is difficult to complete computation of frequency sweep.

The promising and interesting approach to the broadband electromagnetic response over a frequency band without the direct calculation is the data reconstruction method. Asymptotic waveform estimation (AWE) [14], [15], model-based parameter estimation (MBPE) [16]-[18], model order reduction [19], interpolation methods [20]-[24], extrapolation methods [25], and Stoer-Bulirsch algorithm [26], etc., have been developed. However, on the one hand, the above methods in the formulation-domain modeling are based on the fully filled impedance matrix. On the other hand, the methods in the solution-domain modeling suffer from the difficulty of keeping accuracy due to the fast oscillating of the data. For example, AWE is accurate only around the frequency of expansion and is difficult to adaptively choose the expansion points. Furthermore, its accuracy deteriorates beyond a certain bandwidth [27], [28]. Some of these methods in the solution-domain are not suitable for the electrically large targets, nor are they suitable for general targets with complex structure in the real world.

In this paper, a method based on the interpolation technique and fast generating matrix method is developed to solve the wideband scattering problem. In this method, only one fixed mesh grid of the target at the highest frequency is required for all frequency samples at which the scattering will be calculated. The proposed algorithm is implemented in the platform of FGG-FG-FFT to enhance its capability for large problems. Furthermore, the near matrix of FGG-FG-FFT over the frequency band are fast generated via interpolation technique, denoted by FGG-FG-FFT-NMI. In order to fast generate the modified matrices at the three normalized frequency samples and the derivative of the modified matrix at the internal sample, a method for fast filling the near matrix is adopted. It can not only reduce the impedance matrix filling time in the whole frequency band but also accelerate the matrix filling process at frequency interpolation sampling points. Therefore, the speed of the wideband scattering analysis is greatly accelerated.

II. FORMULATIONS AND EQUATIONS

A. Impedance matrix form of the normalized frequency

The radiation and scattering problem of an arbitrary shaped perfectly electric conducting (PEC) object can be formulated by the SIEs such as the electric field integral equation (EFIE) and the magnetic field integral equation (MFIE). Assume that the surface current is expanded in terms of the Rao-Wilton-Glisson (RWG) functions [29]. After applying the Galerkin's procedure, the SIEs are converted into the matrix systems.

The frequency range is $[f_l, f_h]$, i.e., the lowest frequency f_l and the highest frequency f_h. The object surface is supposed to be discretized at f_h. λ_h is the wavelength at f_h. The element with the normalized frequency of the impedance matrix for the EFIE and MFIE is, respectively, expressed as:

$$Z_{ij}^{E}(f_r)=\int_{S_i(\lambda_h)}ds\int_{S_j(\lambda_h)}ds'\Big[\vec{J}_i(\vec{r})\cdot\vec{J}_j(\vec{r}\,')k_r - \nabla_h\cdot\vec{J}_i(\vec{r})\nabla'_h\cdot\vec{J}_j(\vec{r}\,')\frac{1}{k_r}\Big]G(\vec{r},\vec{r}\,')j\eta_0\lambda_h^2, \quad (1)$$

$$Z_{ij}^{M}(f_r)=\Big[\frac{1}{2}\int_{S_i(\lambda_h)}ds\vec{J}_i(\vec{r})\cdot\vec{J}_j(\vec{r}\,')-\int_{S_i(\lambda_h)}ds\vec{J}_i(\vec{r})\cdot\hat{n} \times\int_{S_j(\lambda_h)}ds'\nabla_h G(\vec{r},\vec{r}\,')\times\vec{J}_j(\vec{r}\,')\Big]\lambda_h^2, \quad (2)$$

where, $G(\vec{r},\vec{r}\,')$ denotes the Green's function of free space, which can be expressed as:

$$G(\vec{r},\vec{r}\,')=\frac{e^{-jk_r|\vec{r}-\vec{r}\,'|}}{4\pi|\vec{r}-\vec{r}\,'|}, \quad (3)$$

where $k_r=2\pi f_r$. The normalized frequency $f_r=f/f_h$ varies within $[f_l/f_h,1]$.

Usually, S_i consists of two triangle subdomains; that is, $S_i=S_i^+\cup S_i^-$ and, $\vec{J}_i(\vec{r})$ is defined on a pair of triangles as:

$$\vec{J}_i(\vec{r})=\begin{cases}\vec{J}_i^+(\vec{r})=\dfrac{l_i}{2A_i^+}(\vec{r}-\vec{r}_{io}^+), & \vec{r}\in S_i^+\\ \vec{J}_i^-(\vec{r})=\dfrac{l_i}{2A_i^-}(\vec{r}_{io}^-\vec{r}), & \vec{r}\in S_i^-\end{cases}. \quad (4)$$

For more details of RWG basis functions, readers can refer to the literature [29].

The element for the combined field integral equation (CFIE) can be expressed as:

$$Z_{ij}^{C}=\alpha Z_{ij}^{E}+(1-\alpha)\eta_0 Z_{ij}^{M}, \quad (5)$$

where, $0\le\alpha\le1$.

Here, the following modified matrix element is adopted:

$$\tilde{Z}_{ij}^{S}=\begin{cases}Z_{ij}^{S}f_r e^{jk_r R_{ij}} & S_i\cap S_j=0\\ Z_{ij}^{S}f_r & S_i\cap S_j\neq0\end{cases}, \quad (6)$$

where, the superscript $S=E,M,C$ represents EFIE, MFIE and CFIE. $R_{ij}=|\vec{r}_i-\vec{r}_j|$ is the distance between the centers of the RWG elements S_i and S_j. The interpolation scheme requires three frequency samples within $[f_l, f_h]$, i.e., the lowest frequency f_l, the highest

frequency f_h, and an internal frequency f_{in}.

For the integrity of this paper, the interpolation method is introduced briefly [22]. For convenience, let x_0, x_1, x_2, and x denote the normalized frequencies f_l / f_h, f_{in} / f_h, 1, and f / f_h, respectively. $y(x_i)$ denotes the modified matrix elements at x_i, $i = 0,1,2$; $y'(x_1)$ is the first order derivative of $y(x_1)$ with respect to the normalized frequency. The modified matrices for any normalized intermediate frequencies x are then approximated by a cubic polynomial:

$$y(x) = \sum_{i=0}^{2} y(x_i)\phi_i(x) + y'(x_1)\varphi_1(x), \tag{7}$$

where,

$$\phi_0(x) = \left(\frac{x-x_2}{x_0-x_2}\right)\left(\frac{x-x_1}{x_0-x_1}\right)^2, \tag{8}$$

$$\phi_1(x) = \Theta(x)\left(1-\frac{x-x_1}{x_1-x_0}-\frac{x-x_1}{x_1-x_2}\right), \tag{9}$$

$$\phi_2(x) = \left(\frac{x-x_0}{x_2-x_0}\right)\left(\frac{x-x_1}{x_2-x_1}\right)^2, \tag{10}$$

$$\varphi_1(x) = (x-x_1)\Theta(x), \tag{11}$$

$$\Theta(x) = \left(\frac{x-x_0}{x_1-x_0}\right)\left(\frac{x-x_2}{x_1-x_2}\right). \tag{12}$$

B. The frame of the FGG-FG-FFT

Impedance matrix can be split into two parts:

$$Z^S = (Z^{S-near} - Z^{S-far}) + Z^{S-far} \simeq Z^{S-corr} + Z^{S-far}, \tag{13}$$

where Z^{S-corr} is a sparse matrix, which is obtained by letting the "far elements" of $Z^{S-near} - Z^{S-far}$ become zero. The detail of the matrix Z^{S-far} can be written as:

$$Z^{EFIE-far} = j\eta_0\lambda_h^2(k_r\vec{\Pi}\cdot G\vec{\Pi}^T - \frac{1}{k_r}\Pi_d G\Pi_d^T), \tag{14}$$

$$Z^{MFIE-far} = \lambda_h^2\vec{\Pi}_g\cdot G\vec{\Pi}^T, \tag{15}$$

where $\vec{\Pi}$, Π_d and $\vec{\Pi}_g$ are all sparse matrices, where the head mark "$\rightarrow$" implies matrix elements being 3D vectors; G is a triple Toeplitz matrix related to the Green's function and may be simply called the discrete Green's function; the superscript "T" indicates the matrix transpose. The detail of choice for (14) and (15) in the literatures [11], [12].

C. Fast filling the near matrix

As can be seen from the above, in the FFT-based methods, near matrix elements are calculated directly. It is well known that the calculation of the near matrix accounts for most of solution time for large-scale EM problems. When the RWG function is adopted, it can be found that every integral in (1) and (2) for a matrix element Z_{ij}^S includes a lot of calculations shared by other matrix elements. As is shown in Fig. 1, since a RWG function is defined on a pair of triangles with a common edge, the interaction between the two triangles is in close relation to 9 matrix elements. In the widely used RWG-RWG interaction scheme [29], 9 RWG-RWG interactions over a pair of triangles are independently calculated for generating the corresponding 9 matrix elements. Therefore, that leads to repeated calculations, because the triangle-triangle interactions already calculated are not reusable for the RWG-RWG interactions. Removing these redundant calculations can greatly improve the efficiency of generating matrix. A triangle-triangle scheme was proposed to accelerate filling MoM matrix [30]. However, the method adopted by this paper is different from the method in the literature [30].

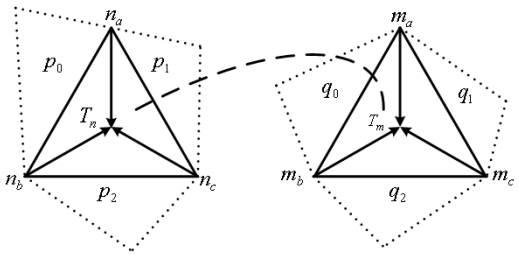

Fig. 1. Triangle-triangle interactions of RWG functions.

The matrix elements of (1) and (2) are both in form of the RWG-RWG interaction. The triangle-triangle interactions of the matrix element of (1) and (2) can be calculated as:

$$Z_{ij} = Z_{S_i^+,S_j^+} + Z_{S_i^+,S_j^-} + Z_{S_i^-,S_j^+} + Z_{S_i^-,S_j^-}. \tag{16}$$

For convenience, the calculation formulae of the four terms in the right hand of (16) are very analogous, so only one needs to be provided. Here, we present a detailed expression of the main parts:

$$\begin{aligned}&\int_{S_i} ds\vec{J}_i(\vec{r})\cdot\int_{S_j}\vec{J}_j(\vec{r}\,')G(\vec{r},\vec{r}\,')ds'\\ &\quad = \frac{l_i l_j}{4}(Q_1 - \vec{r}_{io}\cdot\vec{Q}_2 - \vec{r}_{jo}'\cdot\vec{Q}_3 + \vec{r}_{io}\cdot\vec{r}_{jo}'Q_4)\end{aligned}, \tag{17}$$

where,

$$Q_1 = \frac{1}{A_i A_j}\int_{S_i}\int_{S_j}\vec{r}\cdot\vec{r}\,'G(\vec{r},\vec{r}\,')dsds', \tag{18}$$

$$\vec{Q}_2 = \frac{1}{A_i A_j}\int_{S_i}\int_{S_j}\vec{r}\,'G(\vec{r},\vec{r}\,')dsds', \tag{19}$$

$$\vec{Q}_3 = \frac{1}{A_i A_j}\int_{S_i}\int_{S_j}\vec{r}G(\vec{r},\vec{r}\,')dsds', \tag{20}$$

$$Q_4 = \frac{1}{A_i A_j}\int_{S_i}\int_{S_j}G(\vec{r},\vec{r}\,')dsds', \tag{21}$$

$$\int_{S_i} ds\vec{J}_i(\vec{r})\cdot\hat{n}\times\int_{S_j} ds'\nabla G(\vec{r},\vec{r}')\times\vec{J}_j(\vec{r}') = \frac{l_i l_j}{4}(P_1-\vec{r}_{io}\times\hat{n}\cdot\vec{P}_2-\vec{r}'_{jo}\cdot\vec{P}_3+\vec{r}'_{jo}\times(\vec{r}_{io}\times\hat{n})\cdot\vec{P}_4), \quad (22)$$

where,

$$P_1=\frac{1}{A_iA_j}\int_{S_i} ds\vec{r}\times\hat{n}\cdot\int_{S_j} ds'\nabla G(\vec{r},\vec{r}')\times\vec{r}', \quad (23)$$

$$\vec{P}_2=\frac{1}{A_iA_j}\int_{S_i} ds\int_{S_j} ds'\nabla G(\vec{r},\vec{r}')\times\vec{r}', \quad (24)$$

$$\vec{P}_3=\frac{1}{A_iA_j}\int_{S_i} ds(\vec{r}\times\hat{n})\times\int_{S_j} ds'\nabla G(\vec{r},\vec{r}'), \quad (25)$$

$$\vec{P}_4=\frac{1}{A_iA_j}\int_{S_i} ds\int_{S_j} ds'\nabla G(\vec{r},\vec{r}'). \quad (26)$$

Note that basic integral terms of (17) and (22) which include Q_1, $\vec{Q}_2$, $\vec{Q}_3$, Q_4, P_1, $\vec{P}_2$, $\vec{P}_3$, $\vec{P}_4$ are irrelevant with information of common edge. These integral items can be easily obtained by Gaussian triangle quadrature, and can be shared by multiple matrix elements, which is the reason why the redundant calculations can be removed. Generally, the interactions between a pair of triangles associate with up to 9 matrix elements.

III. NUMERICAL RESULTS

In this section, several numerical examples are given to demonstrate the efficiency and accuracy of FGG-FG-FFT-NMI. The grid spacings are selected to be equal, i.e., $h_x=h_y=h_z=0.25\lambda_h$ at the highest frequency f_h. The expansion order is $M=2$. When necessary, the direct (no interpolation) FGG-FG-FFT, MoM with out-of-core LU solver and IE-ODDM [31] are also employed as the reference.

Example A: A PEC Rectangular Block

Here, we consider the electromagnetic scattering by a PEC rectangular block with dimensions $10\lambda_h(x)\times 3\lambda_h(y)\times 0.5\lambda_h(z)$, as shown in Fig. 2. The incidence angle is $\theta^{in}=0^o,\phi^{in}=0^o$. In such cases, the frequency varies from 6 to 30 GHz. The rectangular block surface is modeled by with 16,644 triangle patches with the average edge size of $0.1\lambda_h$, yielding 24,966 unknowns. The frequency increment of $\Delta f=1$ GHz is considered.

Plotted in Fig. 3 are the RCS results at the scattering direction $(\theta^S,\phi^S)=(60^o,0^o)$ obtained from FGG-FG-FFT-NMI, direct FGG-FG-FFT, and MoM, respectively. It is also worth mentioning that MoM is used. The result at each frequency point is calculated rigorously. It shows that the RCS results computed by FGG-FG-FFT-NMI agree very well with those by direct FGG-FG-FFT and MoM.

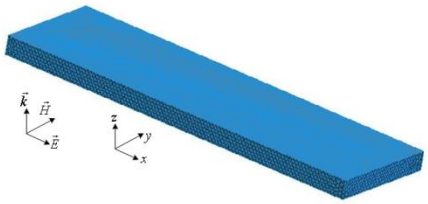

Fig. 2. Geometry of a PEC rectangular block with $10\lambda_h(x)\times 3\lambda_h(y)\times 0.5\lambda_h(z)$.

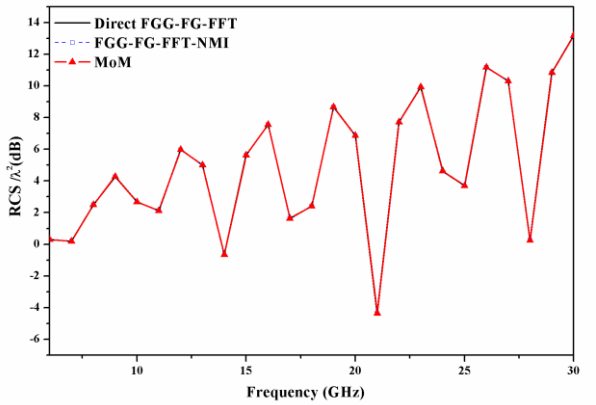

Fig. 3. The RCS of the PEC rectangular block at the scattering direction $(\theta^S,\phi^S)=(60^o,0^o)$ at different frequencies.

As observed from Table 1, the triangle-triangle scheme reduces the CPU time to 12.89% of the time required by the RWG-RWG scheme at 30 GHz. The statistics on the filling time of near matrix are listed in Table 2 at 20 GHz. As shown in Table 2, the CPU time to fill this matrix is cut down. In this example, it costs about 1.27 hours using FGG-FG-FFT-NMI at the whole frequency band, and 3.23 hours using direct FGG-FG-FFT.

Table 1: CPU time for directly calculating the near matrix for the three examples at 30 GHz (in seconds)

Ex.	Method	Time Cost	Time Ratio	Reduced By
A	RWG-RWG	300.3	7.76	87.11%
	Triangle-Triangle	38.7		
B	RWG-RWG	310.3	8.36	88.03%
	Triangle-Triangle	37.1		
C	RWG-RWG	1092.1	7.94	87.41%
	Triangle-Triangle	137.5		

Table 2: CPU time spent of the filling time (in seconds)

Ex.	Method	Z^{near}	Near part In Z^{far}
A	Direct Calculation	300.3	25.5
	Interpolation Scheme	0.24	24.3
B	Direct Calculation	304.7	26.3
	Interpolation Scheme	8.02	26.6
C	Direct Calculation	1130.6	70.4
	Interpolation Scheme	10.3	72.2

Example B: A Metallic 90° Dihedral Corner Reflector

The example deals with a flat metallic structure. The scattering from a metallic 90° dihedral corner reflector as shown in Fig. 4 is considered in a bandwidth from 6 GHz to 30 GHz. The two plates, with the sharing edge being $16\lambda_h$ long in z-direction, are $8\lambda_h$ long in both x- and y-directions. The RCS is computed for a plane wave incident from $\theta^{in}=0^{o}$ and $\phi^{in}=0^{o}$ with the electric field x-direction polarized as is shown in Fig. 4. The surface of the metallic 90° dihedral corner reflector is discretized with about 10 elements per wavelength, yielding 88,045 unknowns. The frequency increment of $\Delta f=1$ GHz is considered.

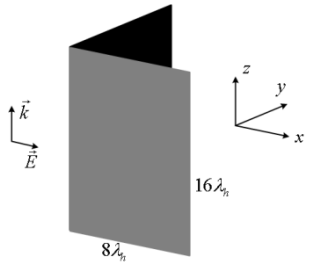

Fig. 4. Geometry of a metallic 90° dihedral corner reflector.

The bistatic RCS at 11 GHz and 25 GHz are compared to the results from direct FGG-FG-FFT, FGG-FG-FFT-NMI and MOM in Fig. 5, respectively. The good agreement in these two figures shows the accuracy of the proposed method in this paper. The variation of RCS with frequency at the scattering direction $\theta^{S}=150^{o}$, $\phi^{S}=0^{o}$, as shown in Fig. 6. It shows that the RCS results computed by FGG-FG-FFT-NMI agree very well with those by direct FGG-FG-FFT and MoM.

Seen from Table 1, the triangle-triangle scheme reduces the CPU time to 11.97% of the time required by the RWG-RWG scheme at 30 GHz. The statistics on the filling time of near matrix are listed in Table 2 at 20 GHz. As shown in Table 2, the CPU time to fill this matrix is cut down by a factor of 37.99. In this example, it costs about 8.17 hours using FGG-FG-FFT-NMI at the whole frequency band, and 10.2 hours using direct FGG-FG-FFT.

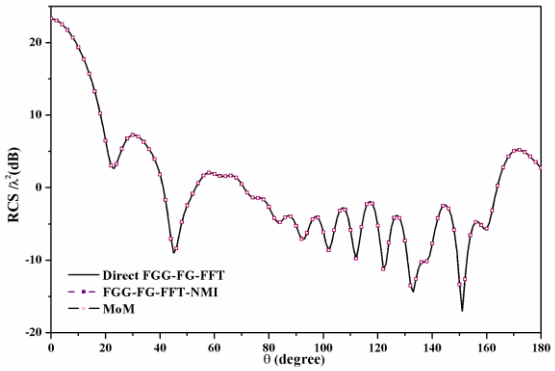

(a) The bistatic RCS curves at 11 GHz

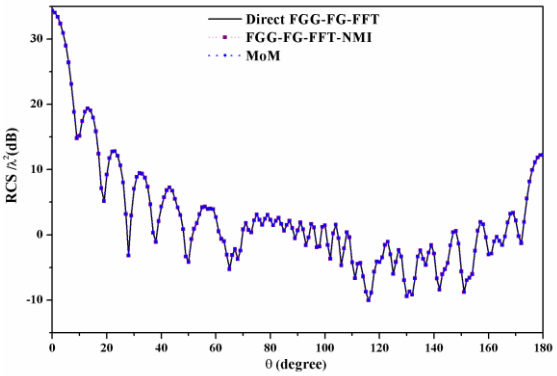

(b) The bistation RCS curves at 25 GHz

Fig. 5. The bistatic RCS curves of a metallic 90° dihedral corner reflector.

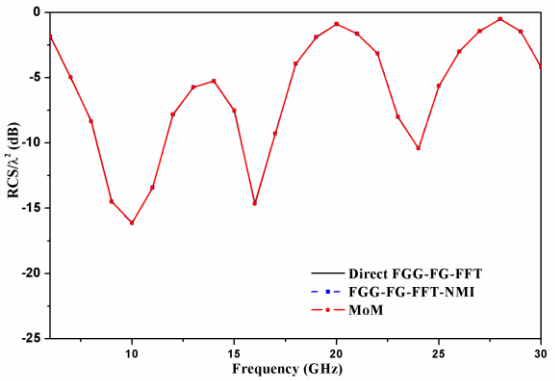

Fig. 6. The RCS of the metallic 90° dihedral corner reflector at the scattering direction $(\theta^{S},\phi^{S})=(150^{o},0^{o})$ at different frequencies.

Example C: A Missile Model

At last, as an example, we consider a missile model. The missile model, $41\lambda_h$ long and $12\lambda_h$ width in the largest dimension as shown in Fig. 7, is simulated using 102,282 unknowns. The frequency is swept from 6 GHz to 30 GHz under the stepping of $\Delta f = 1\,\text{GHz}$.

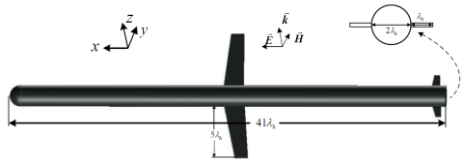

Fig. 7. The PEC missile model.

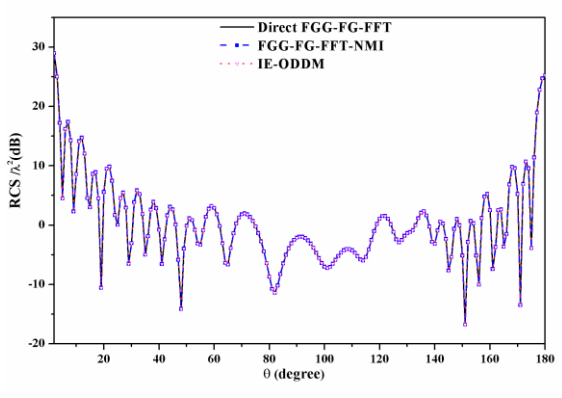

(a) The bistatic RCS curves at 9 GHz

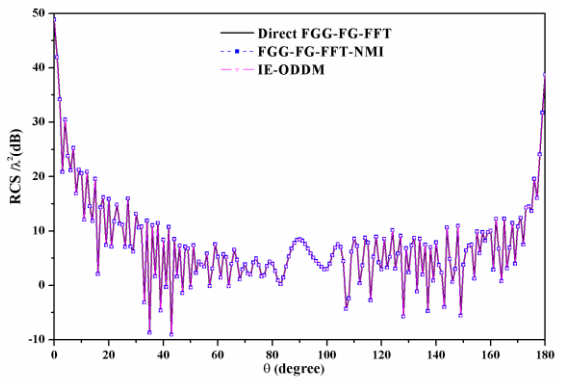

(b) The bistatic RCS curves at 27 GHz

Fig. 8. The bistatic RCS curves of the missile model.

The bistatic RCS at 9 GHz and 27 GHz are compared to the results from direct FGG-FG-FFT, FGG-FG-FFT-NMI and IE-ODDM in Fig. 8, respectively. The good agreement in these two figures shows the accuracy of the proposed method. Figure 9 presents the RCS results at the direction of $(\theta^S, \phi^S) = (80^o, 0^o)$ at different frequencies. It shows that the RCS results computed by FGG-FG-FFT-NMI agree very well with those by direct FGG-FG-FFT. Table 1 lists the CPU time for calculating the near matrix required by the triangle-triangle scheme and RWG-RWG scheme, respectively. At 30GHz, the triangle-triangle scheme reduces the CPU time to 12.59% of that required by the RWG-RWG scheme. The statistics on the filling time of near matrix are listed in Table 2 at 20 GHz. As shown in Table 2, the CPU time to fill this matrix is cut down by a factor of 109.77. In this example, it costs about 7.87 hours using FGG-FG-FFT-NMI at the whole frequency band, and 15.5 hours using direct FGG-FG-FFT. If the frequency increments are smaller, the difference between efficiency of the two methods will be greater. This can also be verified from Table 2.

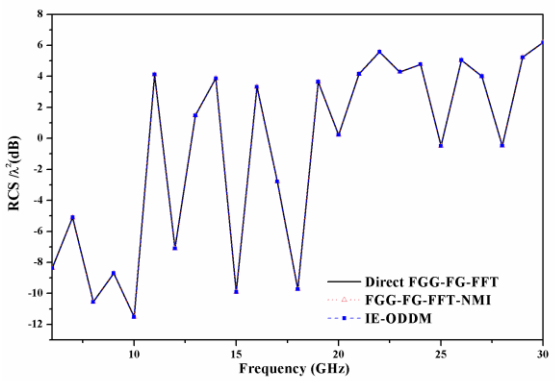

Fig. 9. The RCS of the missile model at the scattering direction $(\theta^S, \phi^S) = (80^o, 0^o)$ at different frequencies.

VI. CONCLUSION

A new fast frequency sweeps method using both the interpolation technique and the fast generating matrix method is proposed. It fuses both the benefits of FGG-FG-FFT and the fast frequency sweeping method based on the interpolation technique and the triangle-triangle scheme. It can not only reduce time in geometrical modeling, but also accelerate the impedance matrix filling process. Thus, it can efficiently accelerate the process of frequency sweeps. The proposed algorithm is not sensitive to both the grid spacing and the expansion order. Numerical experiments validate the accuracy and efficiency.

ACKNOWLEDGMENT

This work was supported by Open Research Program of State Key Laboratory of Millimeter Waves in Southeast University K201718, K201731 and K201928, The Natural Science Foundation of China 61673108, 11801492, The Colleges and Universities Natural Science Foundation in Jiangsu Province 18KJD510010, The Open Project Program of the Key Laboratory of Underwater Acoustic Signal Processing, Ministry of Education UASP1801, The Fundamental Research Funds for the Central Universities 2242016K30013, and

The Natural Science Foundation of Jiangsu Province BK20181050.

REFERENCES

[1] R. F. Harrington, *Field Computation by Moment Methods*. The MacMillian, New York, 1968.

[2] N. Engheta, W. D. Murphy, V. Rokhlin, and M. S. Vassiliou, "The fast multipole method (FMM) for electromagnetic scattering problems," *IEEE Trans. Antennas Propag.*, vol. 40, no. 6, pp. 634-641, June 1992.

[3] J. M. Song, C. C. Lu, and W. C. Chew, "Multilevel fast multipole algorithm for electromagnetic scattering by large complex objects," *IEEE Trans. Antennas Propag.*, vol. 45, no. 10, pp. 1488-1493, Otc. 1997.

[4] W. B. Kong, H. X. Zhou, K. L. Zheng, and W. Hong, "Analysis of multiscale problems using the MLFMA with the assistance of the FFT-Based method," *IEEE Trans. Antennas Propag.*, vol. 63, no. 9, pp. 4184-4188, Sep. 2015.

[5] W. B. Kong, H. X. Zhou, W. D. Li, G. Hua, and W. Hong, "The MLFMA equipped with a hybrid tree structure for the multiscale EM scattering," *International Journal of Antennas and Propagation*, vol. 2014, Article ID 281303, 2014.

[6] X. M. Pan, J. G. Wei, Z. Peng, and X. Q. Sheng, "A fast algorithm for multiscale electromagnetic problems using interpolative decomposition and multilevel fast multipole algorithm," *Radio Sci.*, vol. 47, RS1011, 2012.

[7] E. Bleszybski, M. Bleszynski, and T. Jaroszewicz, "AIM: Adaptive integral method for solving large-scale electromagnetic scattering and radiation problems," *Radio Sci.*, vol. 31, pp. 1225-1251, 1996.

[8] J. R. Phillips and J. K. White, "A precorrected-FFT method for electrostatic analysis of complicated 3-D structures," *IEEE Trans. Computer-Aided Design of Integrated Circuits and Systems*, vol. 16, 1059-1072, 1997.

[9] W. J. Yu, C. H. Yan, and Z. Y. Wang, "Fast multi-frequency extraction of 3-D impedance based on boundary element method," *Microw. Opt. Tech. Lett.*, vol. 50, no. 8, pp. 2191-2197, Aug. 2008.

[10] S. M. Seo and J. F. Lee, "A fast IE-FFT algorithm for solving PEC scattering problems," *IEEE Trans. Magn.*, vol. 41, vol. 5, pp. 1476-1479, May 2005.

[11] J. Y. Xie, H. X. Zhou, W. B. Kong, J. Hu, Z. Song, W. D. Li, and W. Hong, "A novel FG-FFT method for the EFIE," *in Int. Conf. Comput. Problem-Solving (ICCP)*, 2012.

[12] J. Y. Xie, H. X. Zhou, W. Hong, W. D. Li, and G. Hua, "A highly accurate FGG-FG-FFT for the combined field integral equation," *IEEE Trans. Antennas Propag.*, vol. 6, no. 9, pp. 4641-4652, Sep. 2013.

[13] L. J. Jiang and W. C. Chew, "A mixed-form fast multipole algorithm," *IEEE Trans. Antennas Propagat.*, vol. 53, no. 12, pp. 4145-4156, Dec. 2005.

[14] C. J. Reddy, M. D. Deshpande, C. R. Cockrell, and F. B. Beck, "Fast RCS computation over a frequency band using method of moments in conjunction with asymptotic waveform evaluation technique," *IEEE Trans. Antennas Propag.*, vol. 46, no. 8, pp. 1229-1233, Aug. 1998.

[15] R. Bao, A. Q. Wang, and Z. X. Huang, "Fast simulations of electromagnetic scattering from rough surface over a frequency band using asymptotic waveform evaluation technique: horizontal polarization," *J Electromagn. Waves Appl.*, vol. 32, no. 11, pp. 1379-1388, 2018.

[16] E. K. Miller, "Model-based parameter estimation in electromagnetics: Part I. Background and theoretical develop," *IEEE Antennas Propag. Mag.*, vol. 40, no. 1, pp. 42-52, Feb. 1998.

[17] E. K. Miller, "Model-based parameter estimation in electromagnetics: Part II. Applications to EM observables," *IEEE Antennas Propag. Mag.*, vol. 40, no. 2, pp. 51-65, Apr. 1998.

[18] E. K. Mille, "Model-based parameter estimation in electromagnetics: Part III. Applications to EM integral equations," *IEEE Antennas Propag. Mag.*, vol. 40, no. 3, pp. 49-66, June 1998.

[19] V. V. S. Prakash, "RCS computation over a frequency band using the characteristic basis and model order reduction method," i*n Proc. IEEE Antennas Propag. Soc. Int. Symp.*, vol. 4, pp. 89-92, 2003.

[20] E. H. Newman, "Generation of wide-band data from the method of moments by interpolating the impedance matrix," *IEEE Trans. Antennas Propag.*, vol. 36, no. 12, pp. 1820-1824, Dec. 1988.

[21] J. Yeo and R. Mittra, "An algorithm for interpolating the frequency variations of method-of-moments matrices arising in the analysis of planar microstrip structures," *IEEE Trans. Microw. Theory Tech.*, vol. 51, no. 3, pp. 1018-1025, Apr. 2003.

[22] W. D. Li, H. X. Zhou, W. Hong, and T. Weiland, "An accurate interpolation scheme with derivative term for generating MoM matrices in frequency sweeps," *IEEE Trans. Antennas Propag.*, vol. 57, no. 8, pp. 2376-2385, June 2009.

[23] W. D. Li, J. X. Miao, J. Hu, Z. Song, and H. X. Zhou, "An improved cubic polynomial method for interpolating/extrapolating MoM matrices over a frequency band," *Progress in Electromagnetics Research*, vol. 117, pp. 267-281, 2011.

[24] Y. L. Xu, H. Yang, X. Liu, and R. J. Shen, "An interpolation scheme for Green's function and its application in method of moment," *Applied Computational Electromagnetics Society*, vol. 33,

no. 7, July 2018.

[25] Y. Wang, H. Ling, J. Song, and W. C. Chew, "A frequency extrapolation algorithm for FISC," *IEEE Trans. Antennas Propag.*, vol. 45, no. 12, pp. 1891-1893, Dec. 1997.

[26] A. Karwowski, A. Noga, and T. Topa, "Computationally efficient technique for wide-band analysis of grid-like spatial shields for protection against LEMP effects," *Applied Computational Electromagnetics Society*, vol. 32, no. 1, pp. 87-92, Jan. 2017.

[27] H. H. Zhang, Z. H. Fan, and R. S. Chen, "Fast wideband scattering analysis based on Taylor expansion and higher-order hierarchical vector basis functions," *IEEE Antennas Wireless Propag. Lett.*, vol. 14, pp. 579-582, 2015.

[28] G. H. Wang and Y. F. Sun, "Broadband adaptive RCS computation through characteristic basis function method," *Journal of Electrical & Computer Engineering*, vol. 2014, pp. 1-5, 2014.

[29] S. M. Rao, D. R. Wilton, and A. W. Glisson, "Electromagnetic scattering by surfaces of arbitrary shape," *IEEE Trans. Antennas Propag.*, vol. 30, no. 3, pp. 409-418, May 1982.

[30] Y. Zhang, *Electromagnetic Field Parallel Computation*. XDUP, Xi An, 2006. (Chinese).

[31] W. D. Li, W. Hong, and H. X. Zhou, "Integral equation-based overlapped domain decomposition method for the analysis of electromagnetic scattering of 3D conducting objects," *Microw. Opt. Tech. Lett.*, vol. 49, no. 2, pp. 265-274, Dec. 2007.